REPORT DOCUMENTATION PAGE

Form Approved OMB No. 0704-0188

1. REPORT DATE *(DD-MM-YYYY)*	2. REPORT TYPE	3. DATES COVERED *(From - To)*
28-02-2007	Final Performance Report	15-02-2004 -- 31-12-2006

4. TITLE AND SUBTITLE
Development of a Miniaturized Hadamard Transform Time-of-Flight Mass Spectrometer

5a. CONTRACT NUMBER

5b. GRANT NUMBER
FA9550-04-1-0076

5c. PROGRAM ELEMENT NUMBER

6. AUTHOR(S)
Richard N. Zare

5d. PROJECT NUMBER

5e. TASK NUMBER

5f. WORK UNIT NUMBER

7. PERFORMING ORGANIZATION NAME(S) AND ADDRESS(ES)
Department of Chemistry
Stanford University
Stanford, CA 94305-5080

8. PERFORMING ORGANIZATION REPORT NUMBER

9. SPONSORING / MONITORING AGENCY NAME(S) AND ADDRESS(ES)
Air Force Office of Scientific Research
4015 Wilson Blvd., Room 713
Arlington, VA 22203-1954
Dr Michael Berman/NSL

10. SPONSOR/MONITOR'S ACRONYM(S)

11. SPONSOR/MONITOR'S REPORT NUMBER(S)

12. DISTRIBUTION / AVAILABILITY STATEMENT
Approved for public release, distribution unlimited

AFRL-SR-AR-TR-07-0101

13. SUPPLEMENTARY NOTES
None

14. ABSTRACT
This report details advances in theory and technology for the precise deflection of high kinetic energy ion beams using Bradbury-Nielsen gates (BNGs) and their application to high duty cycle miniaturized mass spectrometry. We have developed methods to fabricate BNGs using template assisted manual weaving and silicon-on-insulator microfabrication. These devices have been characterized using ion beam imaging techniques, and the results compared to mathematical models of the deflection process developed for this purpose. A new vacuum-compatible electronic system has been constructed to allow the deflection of ions using BNGs following an arbitrary digital sequence that minimizes the impact of impedance mismatching within the circuit and improves the precision of deflection. The aforementioned advances have been integrated to develop a new form of time-of-flight mass spectrometry that allows for 100% duty cycle detection of a continuous ion beam. Experiments detailing 100% duty cycle operation are described. The statistical advantages to this form of detection over other forms of mass spectrometry in a shot noise dominant environment are presented.

15. SUBJECT TERMS
Mass spectrometry, Bradbury-Nielsen gates, high duty cycle miniaturized mass spectrometry

16. SECURITY CLASSIFICATION OF:			17. LIMITATION OF ABSTRACT	18. NUMBER OF PAGES	19a. NAME OF RESPONSIBLE PERSON
a. REPORT	b. ABSTRACT	c. THIS PAGE		27	Michael Berman
					19b. TELEPHONE NUMBER *(include area code)* 703-696-7781

FINAL PERFORMANCE REPORT

TITLE: Development of a Miniaturized Hadamard Transform Time-of-Flight Mass Spectrometer

GRANT NUMBER: FA9550-04-1-0076

PRINCIPAL INVESTIGATOR: Richard N. Zare
Marguerite Blake Wilbur Professor
of Natural Science
Department of Chemistry

INSTITUTION: Stanford University
Office of Sponsored Research
651 Serra Street
Stanford, CA 94305-4125

1. Introduction

1.1 Technique Description

Time-of-flight mass spectrometry (TOFMS) is perhaps the simplest and most cost-effective form of molecular weight analysis. In traditional TOFMS, an ion packet is accelerated to a known high kinetic energy and pulsed into a field-free drift region. Within this field-free region, the ion packet separates based upon the different velocities of ions having different mass-to-charge ratios. A measurement of an ion's flight time from the initial gating pulse until arrival at the detector determines the ion's mass-to-charge ratio, using proper calibration.

Because TOFMS is inherently a pulsed technique, efficient coupling to a continuous ion source presents a technical challenge. Specifically, while a packet of ions undergoes mass analysis, the continuously evolving ion beam goes unsampled and ions that might otherwise be detected are wasted. Moreover, because a single pulse often contains few ions, the spectra from multiple pulses must be summed to produce a statistically stable and interpretable measure of the ion beam composition. In traditional TOFMS this must be accomplished serially and the process can become time consuming, especially for high mass range analysis where long drift times are required. We have developed a novel TOFMS technique, called Hadamard transform time-of-flight mass spectrometry (HT-TOFMS), in which multiple ion packets are measured simultaneously so that the resulting summed spectra more rapidly converge to a true measure of the ion beam composition.

HT-TOFMS is accomplished through the introduction of pseudorandom pulses of ion packets into the TOF drift region. The Hadamard matrices used to define the pulses are the source for the technique's name. These pulses are generated using a Bradbury-Nielson gate (BNG), which is a set of two interleaved, electrically isolated and independently addressable sets of wires arranged in a plane. When both sets of wires are at equal potential, ions are transmitted though the BNG and their trajectories are unaffected. To modulate the ion beam, voltage pulses of equal magnitude and opposite polarity are applied to the different wire sets, which result in deflection of the beam into two separate branches. One feature of the BNG is that the electric field decays rapidly

along the axis orthogonal to the plane of the gate, allowing a controlled, narrow deflection region. The deflection region ends about one wire spacing away from the plane of the gate.

The key advantages of HT-TOFMS are:

(1) Rapid data acquisition: We have published spectra collected at rates up to 2500 spectra/s over a mass range from 1 to 2000 amu.

(2) 100% duty cycle/high sensitivity: Using patterned anode detection, we have achieved 100% duty cycle measurement independent of the mass range analyzed.

(3) Increased peak height precision: The precision of the peak heights in the mass spectra is improved by the increased duty cycle. This feature is important for studying time-dependent processes, where the intensity changes with time.

(4) Retained instrumental simplicity of TOFMS: The HT-TOFMS retains the cost effectiveness that makes TOFMS an appealing technique. No advanced machining, precision RF power supplies, or high-field magnets are required.

1.2 Objectives

The objectives of this research program were to develop the technology and theoretical understanding necessary to construct a miniaturized HT-TOFMS system.

2. Accomplishments

2.1 Understanding the Effects of Shot Noise and Peak Height Precision[1]

HT-TOFMS is a multiplexing technique that offers high duty cycle for the mass analysis of continuous ion sources. One of the main results of high duty cycle is the increased signal-to-noise ratio (SNR) over conventional on-axis TOFMS. This multiplexing advantage is well-known to be maximized when spectral noise is

[1] Kimmel, J. R.; Yoon, O. K.; Zuleta, I. A.; Trapp, O.; Zare, R. N. Peak Height Precision in Hadamard Transform Time-of-Flight Mass Spectra. *J. Am. Soc. Mass Spectrom.* **2005**, 16, 1117-1130.

independent of signal intensity.[2] However, if the noise is signal-dependent, the noise increases with signal intensity and the SNR can decrease. Thus, characterizing the nature of spectral noise in HT-TOFMS and determining its significance is very important for understanding the technique.

HT-TOFMS is an ion counting technique, which uses a voltage-discriminated multichannel scaler (MCS) to digitize the output of the multichannel plate (MCP) detector. Thus, uncorrelated detector noise (e.g., thermal noise or dark counts) and pulse height distribution from the MCP detector are considered to be negligible. Likewise, any signals with intensity less than the discriminator threshold are ignored so that MCP ringing presents no contribution. Spectral analysis of time traces of total ion current from the electrospray ion source shows that $1/f$ type signal-dependent noise is negligible at normal scan rates. Therefore, the primary cause of the observed baseline noise in HT-TOF mass spectra is the shot noise, which originates from stochastic ion arrivals and its variance is equal to its intensity.

Multiplexing has the advantage of increasing the intensity of recorded peak heights per unit time. For experiments with signal-dependent noise, all peaks are measured above a baseline noise having a magnitude that depends on the populations of all spectral components because the deconvolution spreads out the noise evenly across the spectrum. This behavior is illustrated in the Figure 1, where the mass spectrum of polypropylene glycol has been simulated with ion species removed in order of intensity. Each spectrum contains an inset showing the smallest peak (at 101.1 μs) and the surrounding baseline.

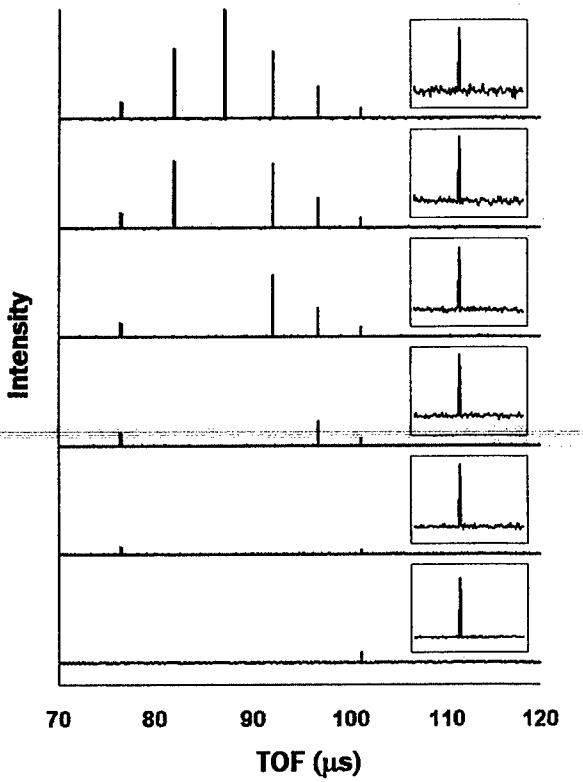

Figure 1. Simulated PPG spectra with dominant peaks removed.

Although the smallest peak has the same intensity in all mass spectra, the baseline

[2] Harwit, M. D.; Sloane, N. J. *Hadamard Transform Optics*; Academic Press: London, 1979.

noise is higher for the spectrum with more neighboring peaks. Thus, we find through simulations and theoretical work that for HT-TOFMS experiments encoded with a sequence that contains N elements, the multiplexing advantage for HT-TOFMS under shot-noise condition is

$$\frac{\mathrm{PHP}_i^{\mathrm{HT}}}{\mathrm{PHP}_i^{\mathrm{TOF}}} = \sqrt{\frac{N}{2} F_i} \qquad (1)$$

Here, F_i is the relative abundance of the ion of interest, and the term peak height precision (PHP) refers to the ratio of the peak height and its standard deviation, whereas SNR is the ratio of the peak height and the standard deviation of the baseline. PHP is used instead of SNR because in the absence of signal-independent noise, the baseline noise can become zero in conventional TOF and SNR would become infinite. Thus, PHP is a better figure of merit for comparison. The equation shows that the multiplexing advantage is $\sqrt{N/2}$ for a single peak, but the advantage is degraded as more peaks are present. In other words, HT-TOFMS is advantageous compared to conventional on-axis TOFMS whenever it is required to measure the peak heights of species present in the ion

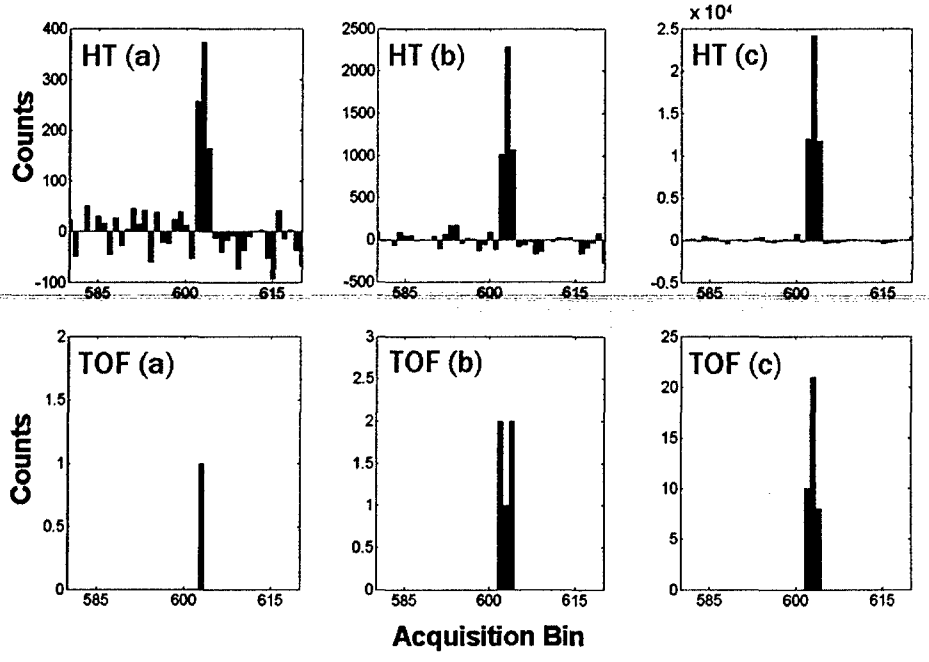

Figure 2. Conventional on-axis TOF and HT-TOF mass spectra of tetrabutylammonium (TBA+) acetate at (a) 500 (b) 50 (c) 10 spectra/s.

beam at percentages greater than 0.1% under typical conditions. To maximize the

advantage of HT-TOFMS, the method should be combined with separations schemes so that the abundance of the ion of interest is not diluted by the presence of other unwanted ions.

This improvement in peak height precision is demonstrated in the Figure 2, which displays simulated HT-TOF and conventional TOF mass spectra at acquisition rates of 500, 100, and 10 spectra per second for a tetrabutylammonium (TBA+) acetate peak that is three bins wide. The peak heights in HT-TOF mass spectra are, on average, three orders of magnitude greater than those of the conventional TOF. Further, Hadamard multiplexing allows true peak shapes (relative peak heights) to be recorded at rates where the conventional experiment detects only a few ions.

This advantage of HT-TOFMS becomes more pronounced as the acquisition rate increases. As a demonstration of these capabilities, Figure 3 shows experimental and simulated mass spectra of TBA^+ under the same conditions as the previous figure but collected at 2500 spectra per second (two 2047-element, 10-MHz passes). The experiment recorded 168 ions in 400 μs, while the equivalent conventional experiment with these ion currents and periodic pulsing would detect an average of 0.185 ions in the same time. This great difference suggests that HT-TOFMS is capable of monitoring transient processes on timescales where precision limits the use of equivalent conventional methods.

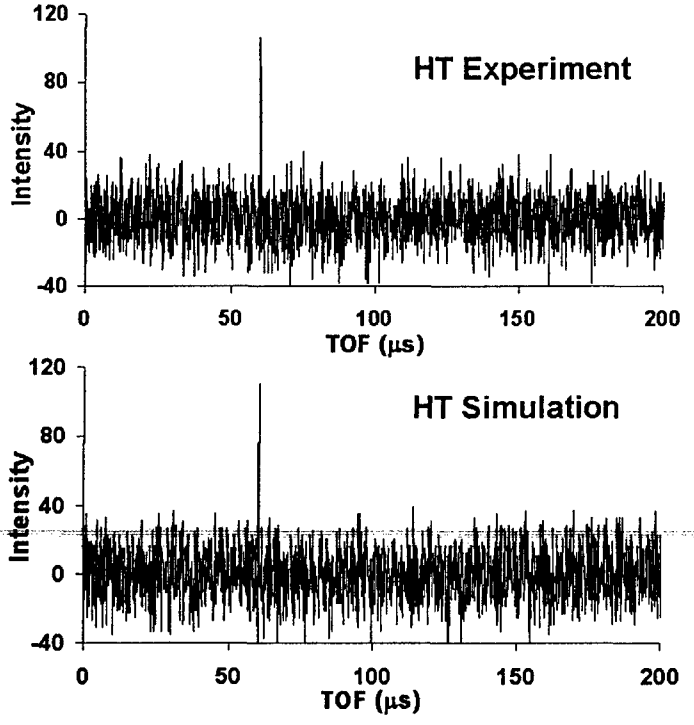

Figure 3. Experimental and simulated HT-TOF mass spectra of TBA+ at an acquisition rate of 2500 spectra/s.

2.2 Development of Beam Modulation Electronics

Although HT-TOFMS offers significant improvement in key figures of merit, its success depends on precision ion modulation. Imperfections in modulation can cause reduction in intensities and spurious peaks in the mass spectra. The majority of this distortion is caused by electronic ringing in the modulation, which appears when the impedances within a network are poorly matched. In HT-TOFMS, the ringing arose from poor impedance matching between the driver circuitry (which amplifies the sequence to the modulation voltage), the ion modulation gate, and the transmission line connecting these two devices. Reconstruction of the instrument was initiated in order to improve the ion modulation by shortening the transmission line and by making the ion modulation gate and driver one unit.

The major changes include new electronics and an aluminum vacuum chamber to house the electronics and dissipate the heat generated by the electronics. The new electronics integrate the ion modulation device and the driver circuitry to remove the transmission line. The custom sequencer is run from a personal computer, where custom and non-symmetric sequences can be applied to the ion modulation gate. Figure 4 compares the modulation sequence traces of the old and new electronics. The improvements in modulation have dramatically improved the quality of acquired mass spectra.

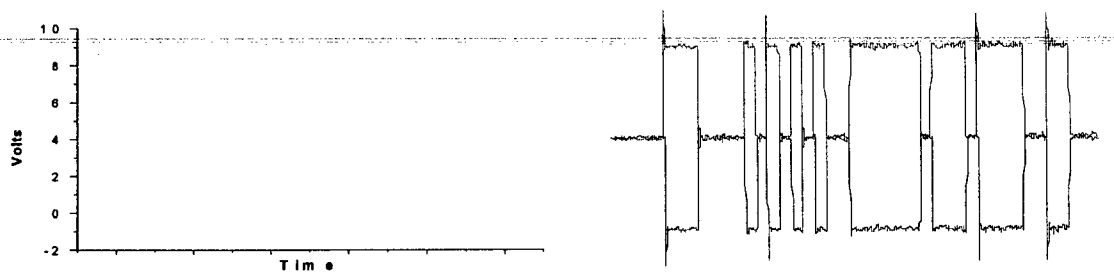

Figure 4. Modulation sequence traces of a) home-built driver board in the 1st generation instrument, b) custom-made driver board in the new instrument (Predicant Biosciences, South San Francisco, CA)

2.3 Development of Sheathless Electrospray Emitters

Electrospray emitters are commonly used to transfer analytes emerging from capillary or chip format separation techniques into the gas phase as charged species for mass detection. Sheathless electrospray and nanospray meet the demand of high sensitivity, low flow rates and reduced peak broadening effects on separations, whereas the widely used and very robust sheath-flow interfaces dilute the eluting analytes with additional liquid and therefore cause decreases in sensitivity at very low flow rates. Electrospray is achieved by applying a high potential (between 2 and 5 kV) to the spray tip, relative to the orifice of the mass spectrometer which represents the counter electrode. In sheathless electrospray emitters the electrical potential is applied to a conductive coating on the outside of the spray tip, which is ideally part of the separation capillary and therefore does not introduce dead-volumes or flow distortions. The use of sheathless electrospray emitters is limited by short lifetimes which are typically up to 100 h for standard electrospray and 6 h for nanospray. This is because of the high electric field strength, leading to sputtering of the coating, and also electrochemical reactions at the interface, mainly oxidation of water in the positive spray mode. In addition, gas formation caused by solvent oxidation and corrosion of the conductive metal surface result in mechanical and oxidative stress on the coating.

We have developed an on-column metal coating procedure for sheathless electrospray emitters based on Justus von Liebig's electroless silver mirror reaction and consecutive electrochemical deposition of gold onto the silver layer.[3] The coating procedure is very straightforward, mild, inexpensive, and can be performed with standard laboratory equipment. Figure 5a shows the SEM picture of the silver-gold coated tip of a sharpened fused silica capillary. The metal surface is very smooth and increases the surface tension of the eluent which improves the formation of a stable Taylor cone (Figure 5b).

A long-term stability investigation of the conductive coating was carried out by continuous electrospray in the positive electrospray mode for 600 hours. The simplicity of the coating procedure and the robustness of the spray tips makes them highly suitable

[3] O. Trapp, E.W. Pearce, J.R. Kimmel, O.K. Yoon, I.A. Zuleta, and R.N. Zare, A Soft On-Column Metal Coating Procedure for Robust Sheathless Electrospray Emitters used in Capillary Elecrophoresis-Mass Spectrometry, *Electrophoresis* **2005**, 26, 1358-1365

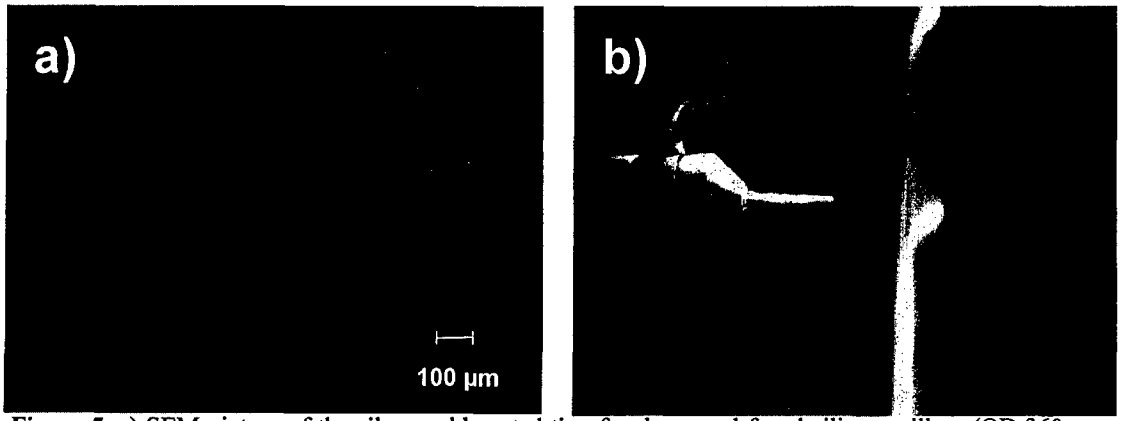

Figure 5. a) SEM picture of the silver-gold coated tip of a sharpened fused-silica capillary (OD 360 µm, ID 75 µm). b) Close-up of a silver-gold coated sheathless electrospray emitter (OD 360 µm, ID 75 µm, flow rate 400 nL/min, spray voltage 2.4 kV)

to couple even delicate wall-coated or monolithic capillary columns with mass spectrometry.

2.4 Derivation of Analytical Expressions to Model the Ion Modulation Process[4]

The most important component of the HT-TOFMS instrument is an ion modulation device, called the Bradbury-Nielson Gate (BNG). The BNG is an ideal deflection plate, capable of transmitting or deflecting an ion beam according to a known binary sequence without changing the flight times of the ions. It consists of two finely spaced, interleaved sets of wire electrodes that are electrically isolated from one another and that lie in a plane perpendicular to the trajectory of the ion beam. Ideally, all ions should be either transmitted or deflected, but in reality, ions can experience partial deflection if the BNG voltage changes as they pass the BNG. Thus, the dynamic behavior of the ion modulation process can affect the performance of HT-TOFMS.

To understand the ion modulation processes, we were able to theoretically derive a simple analytical expression for the deflection angle at the plane of the detector by solving the differential equation for the ion trajectory on the potential energy surface of the BNG. An assumption of the equation is that the kinetic energy of the ion is larger than

[4] Yoon, O. K.; Zuleta, I. A.; Kimmel, J. R.; Robbins, M. D.; Zare, R. N. Duty Cycle and Modulation Efficiency of Two-Channel Hadamard Transform Time-of-Flight Mass Spectrometry. *J. Am. Soc. Mass Spectrom.* **16**, 1888-1901 (2005).

the BNG voltages. Let's assume the BNG is on the y-z plane and an ion is traveling towards the BNG along the x-axis. If the voltages of the BNG are suddenly turned on when the ion is at position (x_0, y_0) and turned off at (x_1, y_0), then, the deflection angle is

$$\tan\alpha(x_0, x_1; y_0) = k\frac{V_p}{V_0}\left[\Theta(x_1, y_0) - \Theta(x_0, y_0)\right] \qquad (2)$$

where $\alpha(x_0, x_1; y_0)$ is the deflection angle and $\Theta(x, y)$ is defined as

$$\Theta(x, y) \equiv \frac{1}{\pi}\left[\arctan\left(\frac{e^{\pi x/d} + \sin(\pi y/d)}{\cos(\pi y/d)}\right) + \arctan\left(\frac{e^{\pi x/d} - \sin(\pi y/d)}{\cos(\pi y/d)}\right)\right] \qquad (3)$$

Also, V_p, V_0, R, and d are BNG voltage, ion kinetic energy, BNG wire radius, and BNG wire spacing, respectively. The constant k is given by

$$k \equiv \frac{\pi}{2\ln\left[\cot\left(\frac{\pi R}{2d}\right)\right]} \qquad (4)$$

and it only depends on the ratio R/d.

To check the accuracy of the analytical equations, ion trajectories through the BNG were simulated using SimIon 3D v7.0. Figure 6 presents the deflection angle plotted against the starting x-position for various wire spacings d. The starting position x_0 is the x-position of the ions relative to the BNG when the voltages are suddenly applied to the BNG wires. The accuracy of the analytical equation is seen by the good fit with the SimIon simulations.

The ion beam is wider than the wire spacing of the BNG and will span several wires. Thus, it is more convenient to use the average of the deflection angles over all y_0 between the wires and remove the y_0 dependence. To find the analytical expression for the average deflection angle, equation 2 has to be integrated over y_0. Instead, this equation was fit to a form almost identical to equation 2 with $y_0 = 0$ and the wire spacing d replaced by an effective wire spacing d_{eff}.

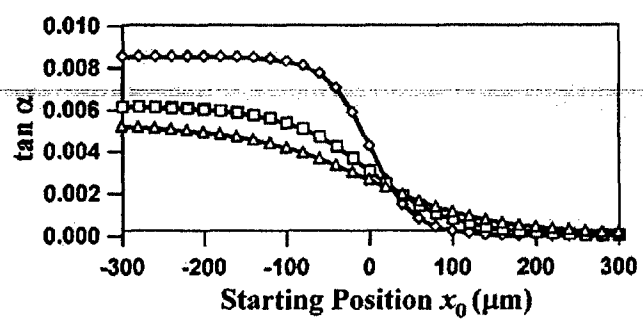

Figure 6. BNG deflection angle versus starting position. Markers are from SimIon simulations and lines are predictions from theory.

$$\tan\alpha_{av}(x_0, x_1) = k\frac{V_p}{V_0}\left[\frac{2}{\pi}\arctan\left(e^{\pi x_1/d_{eff}}\right) - \frac{2}{\pi}\arctan\left(e^{\pi x_0/d_{eff}}\right)\right] \qquad (5)$$

The best fit is achieved when d_{eff} is given by

$$d_{eff} = d\cos\left(\frac{\pi(d-2R)}{4d}\right) \qquad (6)$$

This equation can accurately describe the average dynamic behavior of ions as they are deflected by the BNG. This equation can be extended to other geometry ion modulation gates by changing appropriately k and d_{eff}.

2.5 Fabrication of Bradbury-Nielson Gates

The Bradbury-Nielsen gate is a central part of our ion beam modulation scheme. Two aspects that we are always trying to improve in our instruments are the spacing of the wires in the device as well as the ease and reproducibility of manufacture. We have developed two different methods of BNG fabrication (Figure 7). The first method involves manual weaving of 10 or 20 μm gold-coated tungsten wires on templates that facilitate the alignment of wires. Using this method, BNGs can be produced with wire spacings as small as 50 μm with active areas up to 5 cm without using a microscope. The wire weaving time is about one or two hours. The second method, which involves microfabrication using clean room technology, will be described in section 3.

The two main challenges in fabricating a BNG is precise positioning of wires with a very small spacing and electrical isolation of the two wire sets that are interleaved. In the method developed in this lab, both challenges are overcome by weaving wires onto two templates that have structures that facilitate alignment. The key idea is that the wire positioning is done at a distance much larger than the actual wire spacing. The front face of the template has V-grooves that run vertically with a spacing of twice the desired wire spacing. The top and the bottom surfaces have alignment features that are aligned with the grooves and positioned along a line at a steep angle. Although the grooves are spaced by 100 or 200 μm, the slots are spaced by 1 mm, which is easy to resolve with human eyes. Positioning wires into the matching slots on the top and bottom surfaces guarantees that the wires are inserted into grooves on the template. Thus, precise positioning of wires with a spacing too small to resolve with human eyes is easily achieved without using a

microscope. Then, the two templates are mated face-to-face with a thin insulator between them. The groove structure ensures that the two wire sets are placed between each other in the same plane. Electrical separation of the two wire sets is attained by the insulator.

Figure 8 shows BNGs with wire spacings of 50, 100, 200, and 500 μm that have been fabricated using the template-based method. The fabrication time of a BNG with 10 mm × 15 mm active area and 100 μm wire spacing was about one hour and a BNG with 8 mm × 15 mm active area and 50 μm wire spacing was about two hours. These gates were characterized experimentally by imaging the deflected ion beams and compared to derived analytical expressions (Figure 9 shows one of such images). Table 1 lists some of the characteristics of the BNGs.

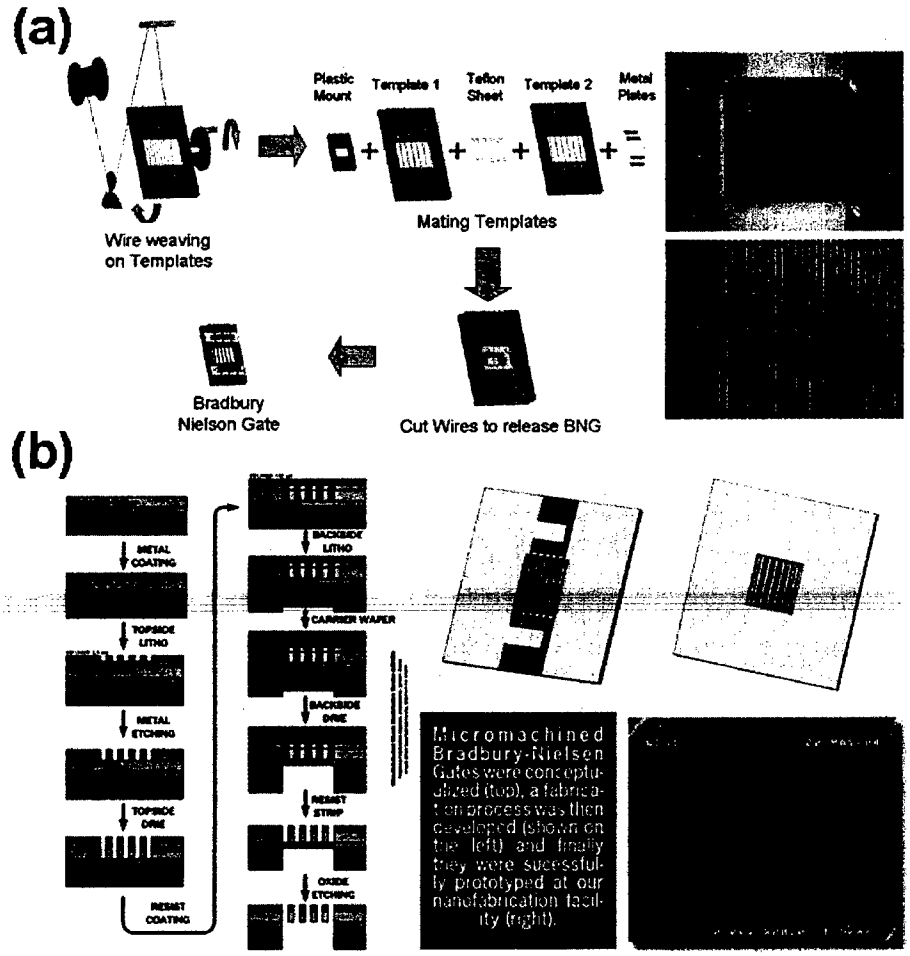

Figure 7. Schematic diagram of two methods for BNG fabrication. (a) Assisted weaving (b) SOI microfacbrication

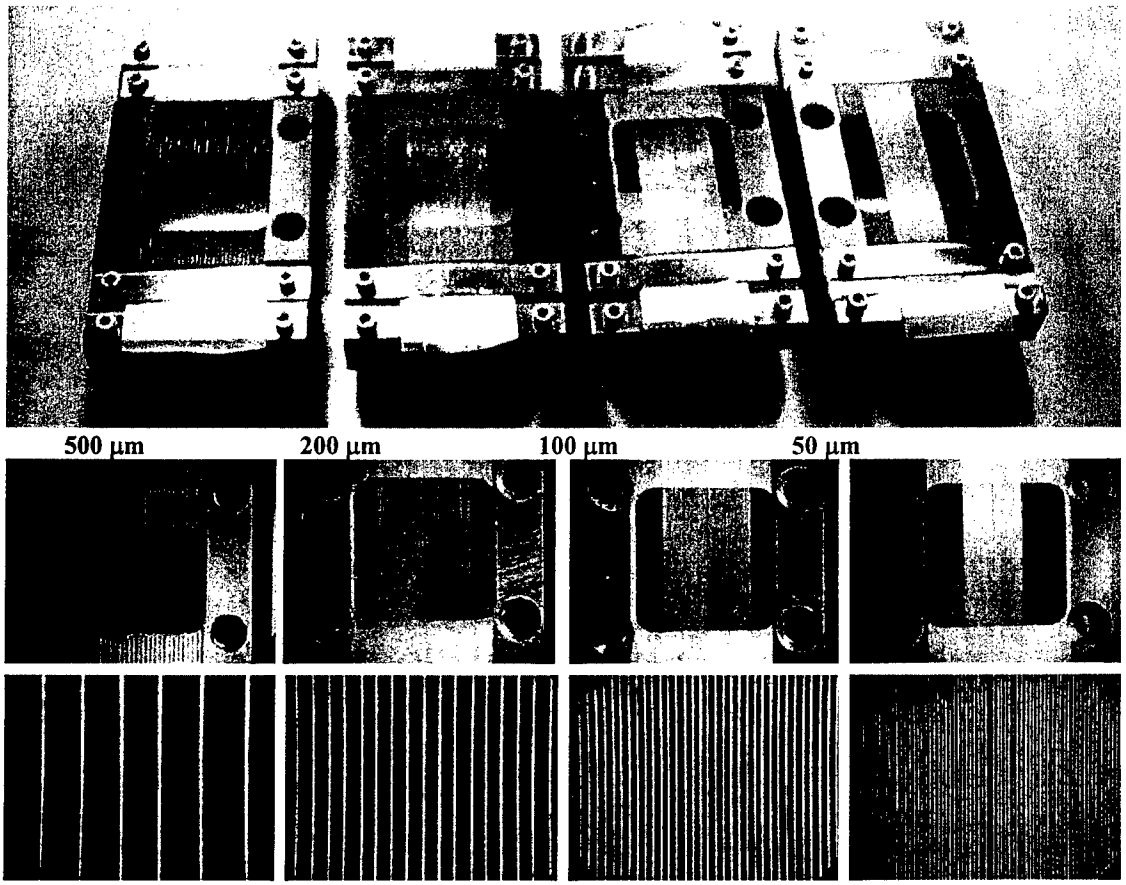

Figure 8. BNGs fabricated using the assisted weaving technique.

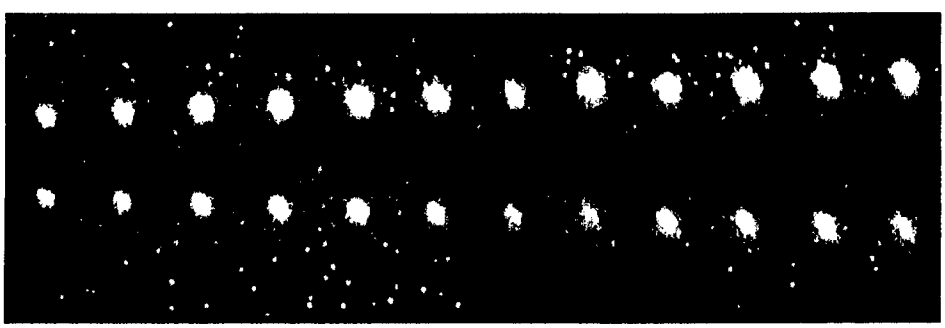

Figure 9. Images of an ion beam deflected into two branches using a BNG.

Table 1. Characteristics of BNGs made using 10 μm diameter gold-coated tungsten wire.

	500 μm	200 μm	100 μm	50 μm
Spacing Std Dev (% Std Dev)	30 μm (6%)	14 μm (7%)	6.5 μm (6.5%)	9 μm (18%)
Transmission	98%	95%	90%	80%
Weaving Time	15 min	30 min	1 hour	2 hours
Capacitance[a] (Theoretical)	10 pF (5 pF)	23 pF (11 pF)	42 pF (29 pF)	80 pF (51 pF)
Theoretical Rise Time[b]	5 ps	10 ps	25 ps	45 ps
Deflection coefficient k[c]	0.378	0.485	0.618	0.852

a. Capacitance of parallel conducting cylinders $C = N\pi\varepsilon_0 L/\cosh^{-1}(d/2r)$
(N=no. of wires, L=wire length, d=wire spacing, r=wire radius)

b. 10%-90% rise time = $2.2RC$, where $R = 0.4\ \Omega$
Note: The rise time of MOSFET driver IC (DEIC420) is 3-4 ns.
Thus, the capacitance of BNG does not affect the rise time.

c. The deflection angle at the detector is $\tan\alpha = kV_p/V_0$, where k is the deflection coefficient, V_p is the voltage applied on the wires, and V_0 is the kinetic energy of the ions. (Ref 4).

2.6 100% Duty cycle experiments

In an attempt to extend the ion efficiency of HT-TOFMS to 100% and to increase the overall performance of the technique, a next generation instrument has been developed using a dual anode detector as shown in Figure 10a. Improvements include new modulation electronics for more precise and faster modulation, new ion optics for a highly focused ion beam with a narrow energy distribution, and home-made software for simultaneous data acquisition and real-time Hadamard transformation. New focusing optics allow us to obtain a highly focused ion beam that can be precisely deflected at the ion beam modulation device with a switching frequency between 5 and 50 MHz. The deflection angle α of the modulated ion beam (Figure 10c) can be controlled by varying the voltage (ΔU) applied to the gate. With sufficient modulation voltage, two spatially resolved modes of the ion beam can be experimentally observed at the detector plane: a centered, focused beam, and the two deflected ion beam braches that arrive above and below the detector center. In order to monitor both spatial modes, we have designed and

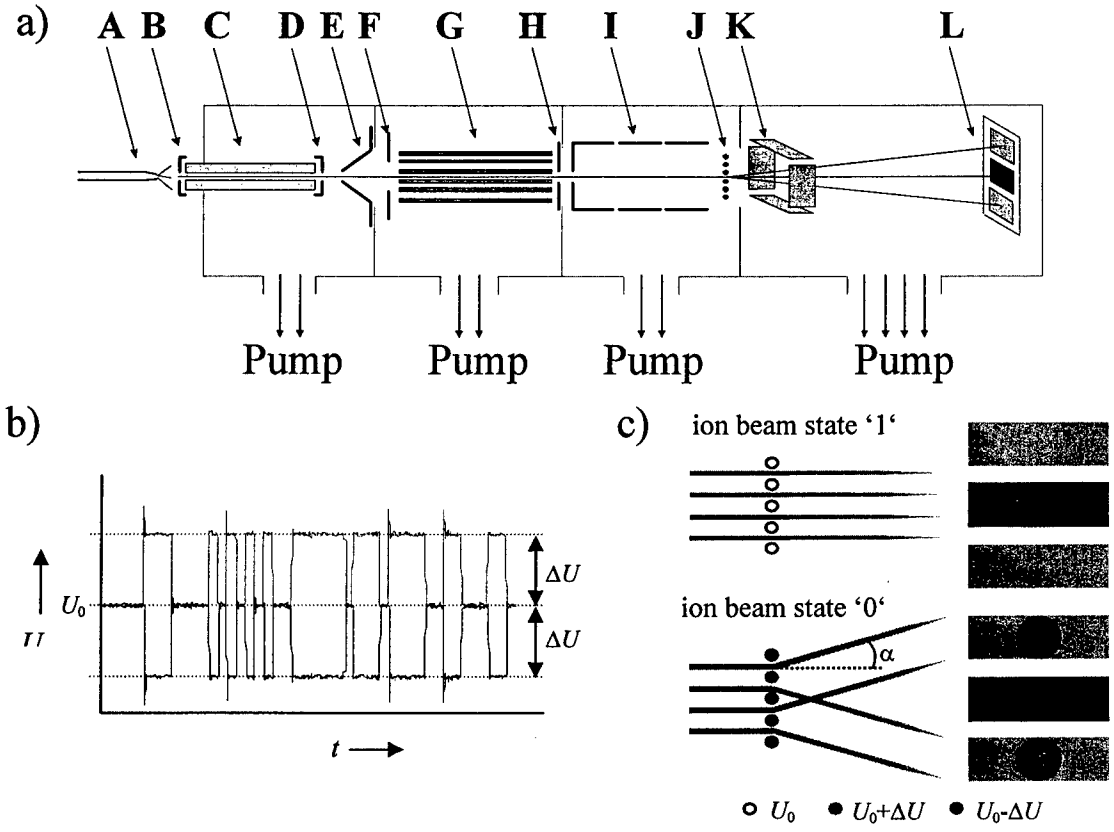

Figure 10. a) Schematic experimental setup of the new HT-TOF mass spectrometer. (A) Electrospray needle, (B) counter electrode, (C) heated glass capillary, (D) capillary exit electrode, (E) skimmer, (F) focusing lens, (G) hexapole, (H) conductance limiting exit lens, (I) Einzel lens, (J) Bradbury-Nielson gate, (K) x,y steering plates, and (L) masked dual anode detector. b) Oscilloscope traces of the positive and negative phases of a Hadamard modulation sequence segment applied to the gate. c) Dual detection scheme demonstrating the ion beam states '0' and '1'.

installed a dual-anode multi-channel plate (MCP) detector with isolated active charge collection areas and a mask that is dimensioned to reflect the spatial profile of the modulated ion beam (Figure 10c).

The ion efficiency of a one-channel HT-TOF mass spectrometer is 50%. Two-channel HT-TOF mass spectrometry involves the simultaneous optimization of paired one-channel HT-TOFMS experiments. Detecting high-quality spectra on the outer channel requires that deflection not only moves ions off the central axis of detection, but also that the deflection is repeatable and well-defined. While the inner channel records the static, focused component of the modulated ion beam, the outer channel detects ions that have undergone a time-dependent deflection. Optimized conditions for both channels require reducing the kinetic energy spread of the ions and matching the images of the

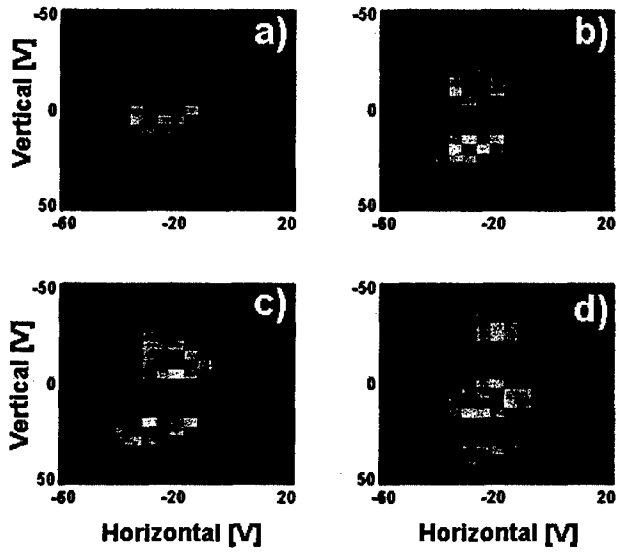

Figure 11. Two-dimensional images of the modulated ion beam obtained by x,y-steering of the undeflected and deflected ion beam across the two detection anodes. a) Undeflected ion beam detected at the inner anode, b) undeflected ion beam detected at the outer anode, c) deflected ion beam (ΔU=13V) detected at the inner anode, and d) deflected ion beam at the outer anode.

deflected and undeflected ion beam modes at the plane of the detector with the detector dimensions. Figure 11 displays the beam images at optimized conditions. The focused ion beam has dimensions comparable to the inner anode and can be moved vertically between the three active areas. The deflected ion beam has two well-defined centers that exist above and below the focused mode.

Figure 12 shows deconvoluted spectra of polypropylene glycol (PPG 450) acquired at the inner and outer anodes. The spectrum of the outer anode is inverted owing to the mathematical formalism of the multiplication of the inverse Hadamard matrix (in our experiment a simplex matrix) with the raw spectrum of the outer anode, where each beam on-state at the inner channel corresponds to a beam off-state at the outer and vice versa. Similar data were collected for analytes across an m/z range of 200 to 2000 amu, including: caffeine, tetrabutylammonium acetate, N-hydroxyethyl-N,N-dimethylbenzyl-ammonium chloride, bradykinin, reserpine, PPG 1000 and gramicidin. In each case, the flight times measured on the two channels were identical, and data subtraction did not require peak matching the two spectra. At faster modulation and acquisition rates the slight difference in the flight paths to the two channels could require a different procedure to match and calibrate data.

With the implemented instrumental modifications, this two-channel detection scheme extends the achievable ion efficiency of HT-TOFMS to 100% and effectively converts TOFMS to a continuous detection technique. Beyond the improved signal-to-noise ratio (SNR), this advance calls for an increase in the data acquisition rate leading to a higher detection speed (several hundred full spectra per second). More generally, this work suggests that temporal and spatial encoding of ion beams combined with multi-channel detection schemes is a promising strategy for increasing the information density of TOFMS experiments.

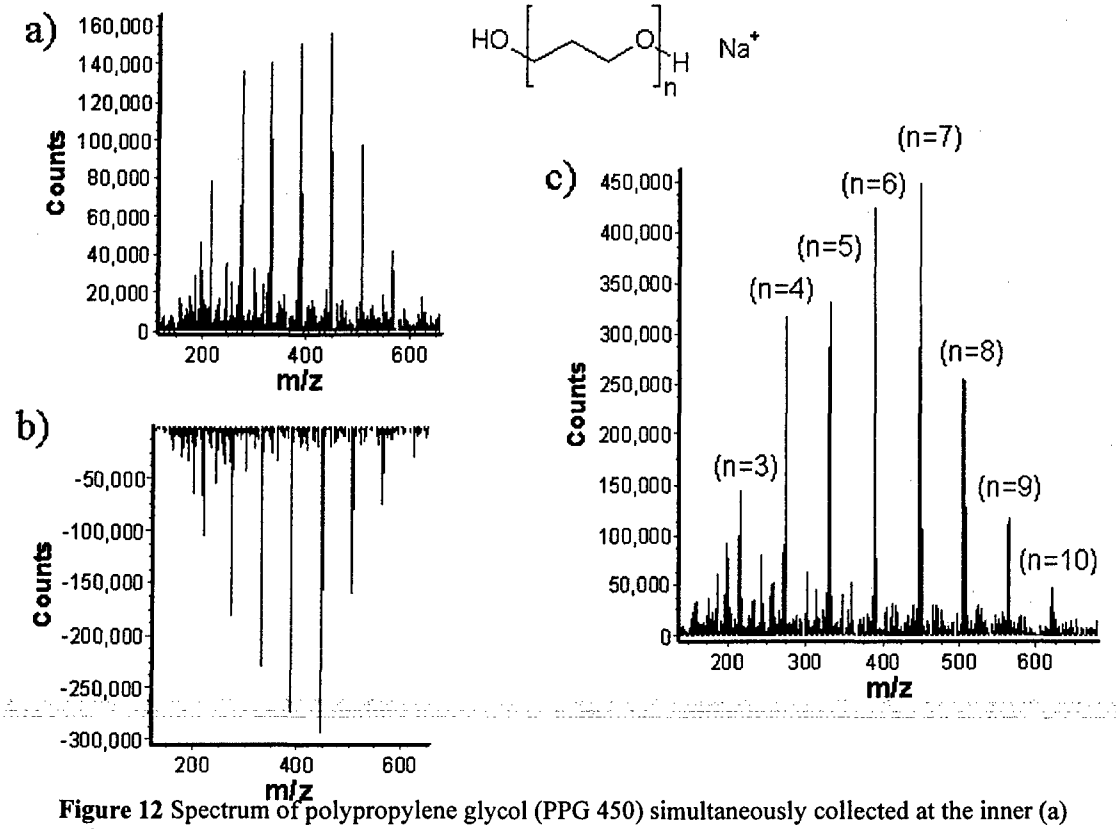

Figure 12 Spectrum of polypropylene glycol (PPG 450) simultaneously collected at the inner (a) and outer (b) anodes of the detector. Spectrum (c) represents the difference of spectrum (a) and spectrum (b) with and experimental improvement of the SNR of 29%. Conditions are 11-bit modulation sequence (2047 elements), 20 MHz modulation frequency, and 30 sec acquisition time.

2.7 Duty cycle and modulation efficiency of the two-channel HT-TOF[4]

In the two-channel (2C) HT-TOFMS, both the transmitted and the deflected ion beams are detected using a patterned dual-anode MCP detector. Thus, 100% duty cycle

can be achieved. 2C-HT-TOFMS involves the simultaneous optimization of paired one-channel (1C) experiments and imposes more stringent conditions to achieve high-quality spectra. Common figures of merit that describe the performance of TOFMS are the signal-to-noise ratio (SNR), sensitivity, and mass resolution. In the current implementation of 2C-HT-TOFMS, the mass resolution is determined by the time width of the data acquisition bin and is not affected significantly by the ion deflection. In contrast, the SNR and sensitivity are directly related to the duty cycle and the ion modulation efficiency, and these depend strongly on the ion modulation process.

The performance of HT-TOFMS depends on well-defined modulation, where the difference between the two deflection states is maximized. In the current HT-TOFMS configuration using a MCP detector, the duty cycle and modulation efficiency are calculated from the measured total ion counts and used to gauge the performance of the modulation process. They are defined as:

$$\text{Duty Cycle} = \frac{\Psi_1 + \Psi_0}{\Psi_{\text{Total}}} \qquad \text{Modulation Efficiency} = \frac{|\Psi_1 - \Psi_0|}{\Psi_1 + \Psi_0} \tag{7}$$

Here, Ψ_1 and Ψ_0 are the total ion counts in the '1' and '0' states of modulation, and Ψ_{Total} is the total ion counts entering the instrument. The duty cycle describes the number of ions that are available for modulation and a higher duty cycle leads to increased sensitivity. Modulation efficiency describes the percentage of those ions that are actually modulated and contribute to peak intensities. The peak height is a function of both the duty cycle and the modulation efficiency, but the baseline noise is only a function of duty cycle. Thus, a high duty cycle is necessary for high sensitivity, but the modulation efficiency must also be maximized to capture the multiplexing advantage. Therefore, the best experimental conditions for HT-TOFMS are those that yield both high modulation efficiency and high duty cycle.

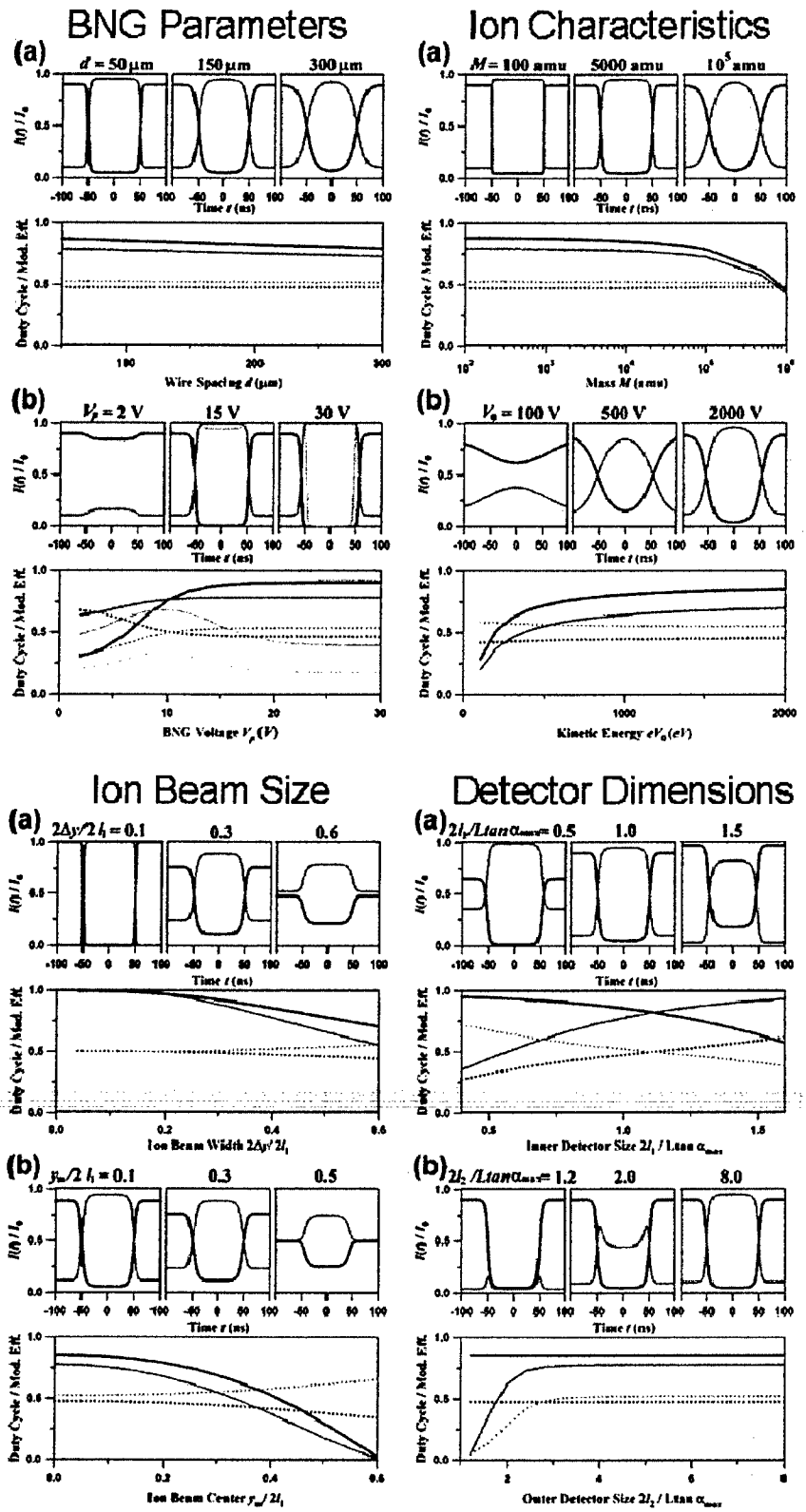

Figure 13. The effects of BNG parameters, ion characteristics, ion beam size, and detector dimensions on duty cycle and modulation efficiency.

Using these definitions, the duty cycles and modulation efficiencies were calculated at various conditions related to the BNG, the ion characteristics, the ion beam size, and the detector dimensions. In Figure 13, the ion current at both detectors in response to a square pulse, duty cycle, and the modulation efficiency are plotted. The black and gray lines correspond to the inner and outer channels, respectively. The solid lines and the dotted lines correspond to modulation efficiencies and duty cycles, respectively. These analyses demonstrate the importance of matching the dimensions of the detector size, ion beam size, and the ion beam deflection angle. The BNG voltage should be chosen such that the maximum deflection by the BNG is larger than the size of the inner detector and smaller than half the size of the outer detector such that all ions are detected. If the outer detector is large enough to detect all deflected ions, 100% duty cycle is always achieved. But, the modulation efficiency needs to be maximized by reducing the inner-anode ion counts in the sequence element 0 and the outer-anode ion counts in the element 1. Tightly focusing the ion beam to be less than half the size of the inner detector and parking the beam in the center of the inner detector help achieve conditions of highest modulation efficiency. Smaller wire spacing for the BNG can also improve the modulation efficiency. Therefore, these theoretical calculations allow qualitative understanding of 2C-HT-TOFMS and permit the optimum conditions to be chosen.

3. Summary of STTR Accomplishments

Our work described here is being followed up in an effort that is being funded in part by the AFOSR. Particularly, better understanding of the Hadamard encoding phenomenon through ion beam imaging, ion population analysis, and the development of continuous-time inverse transforms that enhance resolution is currently being pursued. These studies together with the recently developed and patented microfabricated Beam Modulation Devices (BMDs) are being used to support our efforts to demonstrate small footprint, fast mass spectral analysis using Hadamard Time-of-flight mass spectrometry.

Successful fabrication of BNGs based on silicon monolithic technology was developed jointly with Predicant Biosciences as part of an STTR Phase I contract. Similarly a Phase II contract has been secured with business partner Southwest Scientific,

Inc. to develop a small footprint instrument that features microfabricated ion gates, position sensitive detection, high resolution and real-time, hardware-based modulation and spectral recovery. Below is a short summary of our follow up work, detailed work has been and will be detailed in the respective STTR Progress Reports and Final Reports.

3.1 Microfabrication of Beam Modulation Devices (BMDs)

During the duration of our STTR Phase I contract, we developed mechanical (Figure 14a) and electrical specifications of the new device, simulated the new device and compared it to the performance of a wound-wire BNG; developed a cleanroom process for its micromachining; designed masks for machining the device's features (Figure 14b), and produced prototypes as part of the process development (Figure 14b and 14c). More specifically, we demonstrated a simple fabrication process to create Bradbury-Nielsen-style ion gates using silicon-on-insulator (SOI) wafers.

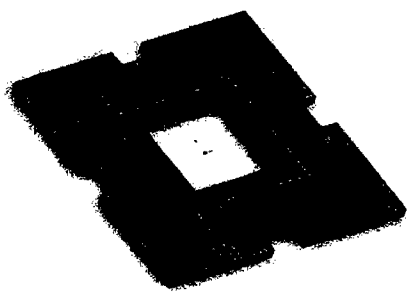

(a)

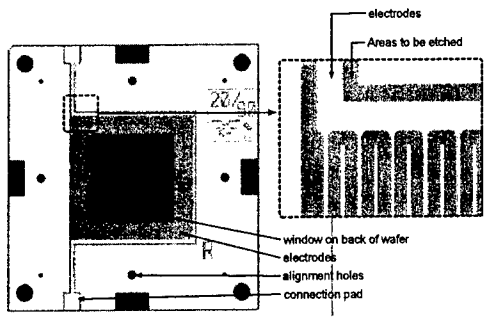

(b)

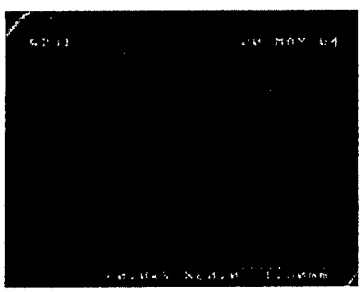

(c)

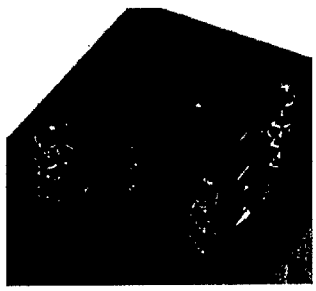

(d)

Figure 14 (a) Mechanical design of the first generation Beam Modulation Device (without wires) and (b) mask design for the same device. (c) SEM image of a sample from our first production batch and (d) several devices mounted in an ion optics stack using self alignment with sapphire spheres.

The characterization of the microfabricated gates is under way and already yielded successful modulation of the ion beam and imaging using a MCP-CCD setup (described in the next section) built for this purpose and for detailed studies of ion modulation and Hadamard optics (Figure 15).

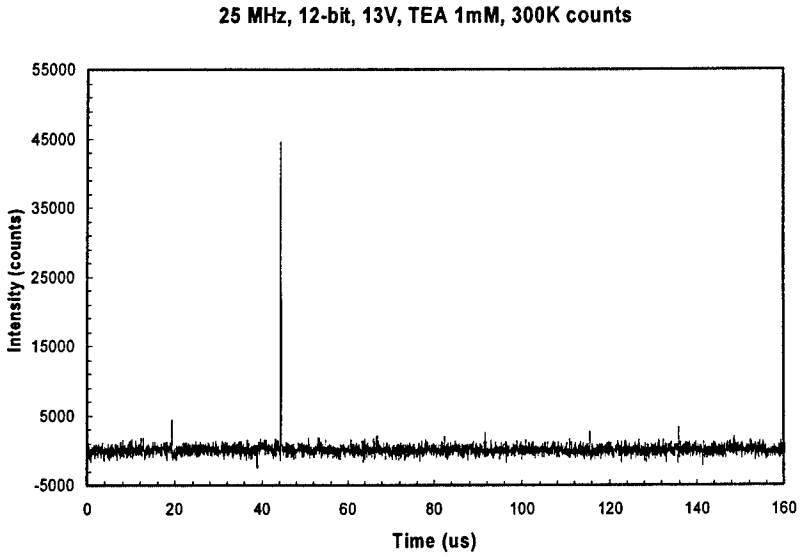

Figure 15. Spectra of tetraethylammonium ion using a microfabricated gate in our current setup.

3.2 Prototype for performance assessment and other novel studies

Based on the progress made on the production of micro-fabricated Bradbury-Nielsen gates, and the need for improved resolution, portability and high spectral acquisition rate, we have constructed a prototype to assess and demonstrate key advantages of Hadamard time-of-flight mass spectrometry. Specifically, this instrument incorporates arbitrary waveform modulation and a position sensitive detection scheme that supports our development of novel, faster and higher resolution operation schemes and enables us to do fundamental studies of ion modulation phenomena.

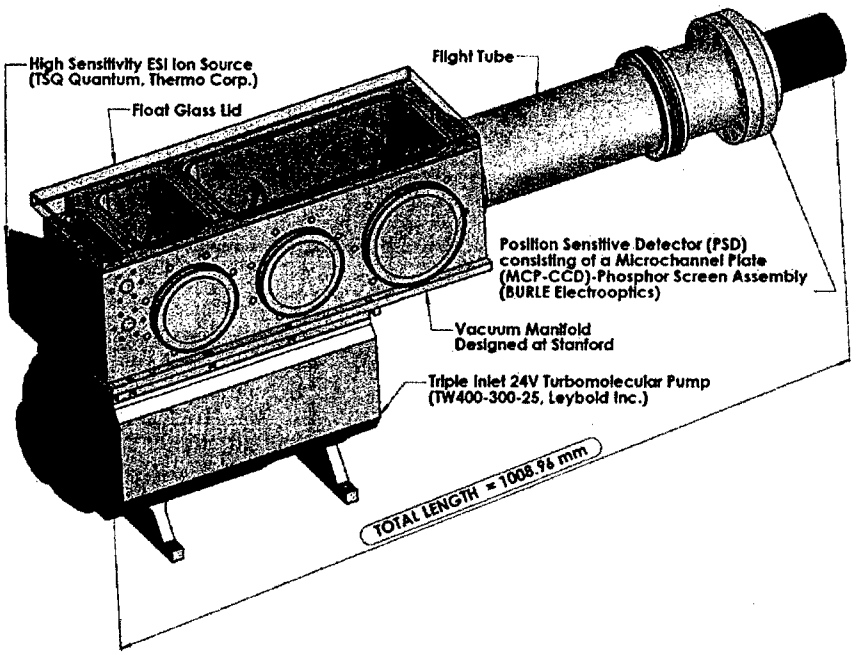

Figure 16. Mechanical rendering of the prototype under construction at Stanford University. Note that the overall length is for the variant for use in the laboratory for development work, actual field-ready units will have shorter flight tubes.

A vacuum manifold houses the electrospray ion source, ion transfer and accelerations optics, Hadamard modulation electronics, a linear flight tube and a position sensitive MCP-Phosphor-CCD detector (Figure 16). The pumping system is comprised of a triple stage hybrid pump that boasts a rugged drag stage that can run at elevated foreline pressures, relaxing pumping requirements significantly. Its imaging capabilities enable optimized operation of linear and reflector mode configurations in 100% duty cycle mode for the first time, while arbitrary modulation enables direct comparison with conventional mode as well as novel operation schemes, again, for the first time. Also, signal processing studies of the modulation process have been carried over to develop a dedicated high resolution deconvolution scheme.

4. Personnel Supported

Richard N. Zare, Principal Investigator
Oliver Trapp, Postdoctoral Research Associate
Joel R. Kimmel, Graduate Student
Oh Kyu Yoon, Graduate Student
Ignacio A. Zuleta, Graduate Student
Matthew D. Robbins, Graduate Student

5. Publications

5.1 Refereed Publications

O. Trapp, J.R. Kimmel, O.K. Yoon, I.A. Zuleta, F.M. Fernandez, and R.N. Zare, "Continuous Two-Channel Time-of-Flight Mass Spectrometric Detection of Electrosprayed Ions," *Angew. Chem. Int. Ed.* **2004**, 43, 6541-6544.

O. Trapp, E.W. Pearce, J.R. Kimmel, O.K. Yoon, I.A. Zuleta, and R.N. Zare, "A Soft On-Column Metal Coating Procedure for Robust Sheathless Electrospray Emitters used in Capillary Elecrophoresis-Mass Spectrometry," *Electrophoresis* **2005**, 26, 1358-1365.

J.R. Kimmel, O.K. Yoon, I.A. Zuleta, O. Trapp, and R.N. Zare, "Peak Height Precision in Hadamard Transform Time-of-Flight Mass Spectra," *J. Am. Soc. Mass Spectrom.* **2005**, 16, 1117-1130.

O. K. Yoon, I. A. Zuleta, J. R. Kimmel, M. D. Robbins, and R. N. Zare, "Duty Cycle and Modulation Efficiency of Two-Channel Hadamard Transform Time-of-Flight Mass Spectrometry," *J. Am. Soc. Mass Spectrom.* **16**, 1888-1901 (2005).

5.2 Doctoral Theses

J.R. Kimmel. Continuous, Multiplexed Time-of-Flight Mass Spectrometry of Electrosprayed Ions, Stanford University, Stanford, CA, December 2004.

6. Inventions

6.1 Patents Awarded

Richard N. Zare, Facundo M. Fernandez, Joel R. Kimmel, Oliver Trapp, "Gating device and driver for modulation of charged particle beams" U.S. Patent 7,067,803, June 27, 2007

I. A. Zuleta, R. N. Zare "Microfabricated Beam Modulation Device" U.S. Patent 7,176,452, Feb 13, 2007.

6.2 Patents Pending

Oh Kyu Yoon, Richard N. Zare, "Fabrication of Bradbury-Nielson Gates with Templates having Wire Insertion Features having Enhanced Spacing" Filed 2006.

7. Presentations

Poster Presentation. O. Trapp, J.R. Kimmel, O.K. Yoon, I.A. Zuleta, R.N. Zare Hadamard-Transform Time-of-Flight Mass Spectrometry: A Potential Detector for Capillary Format Separations. 17th International Symposium on Microscale Separations and Analysis (HPCE 2004), February 8-12, 2004, Salzburg, Austria.

Poster Presentation. Joel R. Kimmel, Oliver Trapp, Oh Kyu Yoon, Ignacio A. Zuleta, Facundo M. Fernandez, Richard N. Zare "Two-channel Hadamard Transform Time-of-flight Mass Spectrometry" 52nd ASMS Conference on Mass Spectrometry, ThPG116, May, 23-27, 2004, Nashville, TN, USA

Poster Presentation. Ignacio A. Zuleta, Joel R. Kimmel, Oliver Trapp, Oh Kyu Yoon, Richard N. Zare "Design and Preliminary Studies on a full Duty Cycle, Multi-anode Multiplexing Time-of-flight Experiment" 52nd ASMS Conference on Mass Spectrometry, MPH126, May 23-27, 2004, Nashville, TN, USA

Poster Presentation. Oh Kyu Yoon, Joel R. Kimmel, Oliver Trapp, Ignacio A. Zuleta, Richard N. Zare "Iterative Estimation and Inversion of Hadamard Modulation in Time-of-flight Mass Spectrometry" 52nd ASMS Conference on Mass Spectrometry, MPH094, May 23-27, 2004, Nashville, TN, USA

Poster Presentation. O.K. Yoon, J.R. Kimmel, I.A. Zuleta, and R.N. Zare, "Detection of Transient Species in Hadamard Transform Time-of-Flight: Peak Height Precision, Duty Cycle, and Modulation Efficiency," 53rd ASMS Conference on Mass Spectrometry, MP274, June 5–9, 2005, San Antonio, TX, USA.

Poster Presentation. I.A. Zuleta, O.K. Yoon, and R.N. Zare, "Electrospray Ionization Time-of-Flight Mass Spectrometry with Microfabricated Beam Modulation Devices," 53rd ASMS Conference on Mass Spectrometry, MP271, June 5–9, 2005, San Antonio, TX, USA.

Poster Presentation. I.A. Zuleta, M.D. Robbins, O.K. Yoon, and R.N. Zare, "Electrospray Ionization Time-of-Flight Mass Spectrometry with Microfabricated Beam Modulation Devices and an MCP-CCD Camera," 2005 AFOSR Contractors Meeting in Molecular Dynamics and Theoretical Chemistry, May 22-24, 2005, Monterey, CA, USA

Poster Presentation. O.K. Yoon, I.A. Zuleta, M.D. Robbins, and R.N. Zare, "Duty Cycle and Modulation Efficiency of Two-channel Hadamard Transform Time-of-flight Mass Spectrometry," 2005 AFOSR Contractors Meeting in Molecular Dynamics and Theoretical Chemistry, May 22-24, 2005, Monterey, CA, USA

Poster Presentation. O.K. Yoon, M.D. Robbins, I.A. Zuleta, G.K. Barbula and R.N. Zare, "Fragmentation Modulation Mass Spectrometry," 2006 AFOSR Contractors Meeting in Molecular Dynamics and Theoretical Chemistry, June 5-7, 2005, Arlington, VA, USA

Poster Presentation. M.D. Robbins, Y. Luo, G.K. Barbula, O.K. Yoon, I.A. Zuleta and R.N. Zare, "Open-Channel Silicon-Based Electrospray Emitter Tips for Coupling with PDMS Microfluidic Systems," 2006 AFOSR Contractors Meeting in Molecular Dynamics and Theoretical Chemistry, June 5-7, 2005, Arlington, VA, USA

Poster Presentation. O.K. Yoon, I.A. Zuleta, M.D. Robbins, G.K. Barbula and R.N. Zare, "Simple Template-Based Method to Fabricate Bradbury-Neilson Gates and Applications to Mass Spectrometry" 54th ASMS Conference on Mass Spectrometry, MP197, May 28–June 1, 206, Seattle, WA, USA.

Poster Presentation. M.D. Robbins, Y. Luo, G.K. Barbula, O.K. Yoon, I.A. Zuleta and R.N. Zare, "Open-Channel Silicon-Based Electrospray Emitter Tips for Coupling with PDMS Microfluidic Systems," 54th ASMS Conference on Mass Spectrometry, ThP 109, May 28–June 1, 206, Seattle, WA, USA.

Poster Presentation. I.A. Zuleta, O.K. Yoon, M.D. Robbins, G.K. Barbula and R.N. Zare, "An Ion-Imaging ESI Hadamard Time-of-Flight (HT-TOF) Mass Spectrometer for Studies on Modulation of Charged Particle Beams and Other Fundamental Processes," 54th ASMS Conference on Mass Spectrometry, WP277, May 28–June 1, 206, Seattle, WA, USA.